Vol. 698: 41–54, 2022
doi: 10.3354/meps14158

MARINE ECOLOGY PROGRESS SERIES
Mar Ecol Prog Ser

Published October 6

# Phosphomonoesterase and phosphodiesterase activities and their regulation during dinoflagellate blooms under different external phosphate conditions

**Kaixuan Huang[1], Zhou Wang[1], Jinzhou Tan[1], Dazhi Wang[2], Xinfeng Dai[3,4], Jingyi Cen[1], Linjian Ou[1,*], Songhui Lu[1]**

[1]Research Center of Harmful Algae and Marine Biology, and Key Laboratory of Eutrophication and Red Tide Prevention of Guangdong Higher Education Institutes, Jinan University, Guangzhou 510632, PR China

[2]State Key Laboratory of Marine Environmental Science, and College of the Environment and Ecology, Xiamen University, Xiamen 361005, PR China

[3]Key Laboratory of Marine Ecosystem Dynamics, Second Institute of Oceanography, Ministry of Natural Resources, Hangzhou 310012, PR China

[4]Fourth Institute of Oceanography, Ministry of Natural Resources, Beihai 536000, PR China

ABSTRACT: Phosphatases play a crucial role in recycling organic phosphorus and determining primary production and phytoplankton communities in seawater, especially in phosphate-depleted coastal waters. The present study analyzed spatiotemporal variation in phosphomonoesterase (PMEase) activity (PMEA) and phosphodiesterase (PDEase) activity (PDEA) during 2 dinoflagellate blooms occurring in 2 coastal areas of Fujian Province, East China Sea, which differed in external phosphate conditions. Together with environmental variables and with a specific focus on the availability of different phosphorus forms in the seawater, the regulation of both phosphatases was studied. The results showed that dissolved organic phosphorus (DOP) was the major phosphorus source during blooms, especially in phosphate-depleted environments. Labile DOP accounted for more than 50% of DOP, of which phosphomonoester (PME) and phosphodiester (PDE) accounted for 75–94% and 6–25%, respectively. PMEA and PDEA were highly correlated, both increasing during blooms with a fixed PMEA:PDEA ratio of 2.5 under external phosphate conditions at both sites. Both PMEA and PDEA were negatively correlated with dissolved inorganic phosphorus (DIP) when phosphate was depleted, but positively correlated with DOP regardless of external phosphate conditions. During dinoflagellate blooms, temperature and phytoplankton biomass were the dominant variables determining both phosphatase activities under phosphate-depleted conditions, whereas the availability of DOP was the dominant variable determining both phosphatase activities under phosphate-replete conditions. This study suggests the importance of phosphatases in recycling DOP, and indicates similar regulation of PMEA and PDEA during dinoflagellate blooms.

KEY WORDS: Phosphatase · Dissolved organic phosphorus · *Prorocentrum donghaiense* · *Karlodinium digitatum* · East China Sea



## 1. INTRODUCTION

Phosphorus is a critical element for microorganisms and plays a crucial role in biogeochemical cycles in aquatic environments (Björkman 2014, Karl 2014). However, in many oceanic (Mills et al. 2004, Lomas et al. 2010, Reinhard et al. 2016) and coastal (Harrison et al. 1990, Liu et al. 2016, Malone & Newton 2020) environments, phosphorus is a limiting nutrient, and thus affects primary production and

*Corresponding author: torangeou@jnu.edu.cn

ecosystem structure. When phosphate is scarce, the availability of dissolved organic phosphorus (DOP) becomes important (Karl & Yanagi 1997, Dyhrman 2016). In coastal waters, DOP accounts for 0 to 50% of the total dissolved phosphorus (TDP) pool (Benitez-Nelson 2000), whereas in the open ocean, the contribution of DOP to TDP may be as high as 75% (Karl & Yanagi 1997). In some marine environments, DOP is multiple times greater than dissolved inorganic phosphorus (DIP) (Benitez-Nelson 2000, Suzumura & Ingall 2004). Phosphate esters (including phosphomonoester, PME, and phosphodiester, PDE) and phosphonates are the main components of DOP (Kolowith et al. 2001, Karl 2014). While phosphonates are refractory and only available to some prokaryotes (Dyhrman 2016, Lin et al. 2016), phosphate esters, which account for 75% of the DOP pool, are much more labile and available to most microorganisms (Kolowith et al. 2001, Karl 2014).

PME is the most abundant phosphate ester in marine environments (Karl & Yanagi 1997, Kolowith et al. 2001), and on average, 66% of DOP in surface waters is biodegradable PME (Benitez-Nelson 2000). Although PME is studied more than PDE, the few available studies on PDE suggest that its concentration, such as in nucleotides and phospholipids, might be similar to or in some cases even higher than that of PME in seawater; thus, PDE is also an important phosphorus source for microorganisms (Suzumura et al. 1998, Yamaguchi et al. 2019). In marine environments, the mineralization of PME and PDE involves a series
of extracellular enzymes, such as phosphomonoesterase (PMEase), phosphodiesterase (PDEase), and 5′-nucleotidases (Benitez-Nelson 2000, Dyhrman 2016). Most investigations of phosphatase hydrolysis of marine DOP have focused on PMEase, especially alkaline phosphatase (Karl 2014, Dyhrman 2016), and there are many studies on the dynamics of PMEase activity (PMEA) (Davis & Mahaffey 2017, Martin et al. 2018, Mo et al. 2020), PMEase classification and characteristics (Ou et al. 2010, 2020, Ghyoot et al. 2015, Lidbury et al. 2022), PMEase biogeography (Srivastava et al. 2021, Lidbury et al. 2022), and PMEase regulation (Sebastián et al. 2004, Duhamel et al. 2010, Qin et al. 2021). PMEase has been suggested to be crucial in regulating recycling of organic phosphorus, and thus might determine primary production or even interspecific competition between phytoplankton when phosphate is limited (Cembella et al. 1982, Davis & Mahaffey 2017). Available field studies have shown that PMEase and PDEase hydrolyze different components of DOP and that both phosphatases play important roles in recycling DOP (Sato et al. 2013, Accoroni et al. 2017, Yamaguchi et al. 2021). The regulation of PDEase activity (PDEA) seems more complicated than that of PMEA (Yamaguchi et al. 2021). Monocultures of some algal species can utilize PDE as the sole phosphorus substrate through hydrolysis of PDEase (Yamaguchi et al. 2014, Ellwood et al. 2020, Yamaguchi et al. 2020, Huang et al. 2021). Thus, considering the amount of PDE in seawater and differences in hydrolysis of PME and PDE, a better understanding of PDEA and its regulation is needed.

Phosphorus is a potential limiting factor and is crucial to the regulation of dinoflagellate blooms in the East China Sea (Li et al. 2011, Zhou et al. 2017, Lu et al. 2022). Several studies have investigated PMEA during dinoflagellate blooms to analyze the phosphorus status of bloom-causing species (Huang et al. 2007, Ou et al. 2020) and the importance of DOP through PMEase hydrolysis (Huang et al. 2007, Qin et al. 2021). However, to date, the relative importance of PME and PDE and their hydrolysis through PMEase and PDEase during blooms remain largely unknown. In the spring of 2019, 2 dinoflagellate blooms caused by *Prorocentrum donghaiense* (also identified as *P. obtusidens*) occurred in the coastal waters of Sansha and Lianjiang, Fujian Province, China. We determined concentrations of PME and PDE using enzymatic hydrolysis analyses, and studied spatiotemporal variations in PMEA and PDEA and their regulation by environmental variables. The most interesting finding was that one of the dinoflagellate blooms occurred at a relatively high phosphate concentration (>0.30 µmol $l^{-1}$ at most stations), whereas the other bloom occurred at a low phosphate concentration (<0.10 µmol $l^{-1}$ at most stations). Hence, it was possible to compare the dynamics of the 2 phosphatase activities and their regulation under contrasting external phosphate conditions with the same experimental conditions for enzymatic assays. The objective of the study was to improve understanding of the bioavailability of different forms of DOP (PME and PDE), phosphatase (PMEase and PDEase) activity dynamics, and phosphatase activity regulation during dinoflagellate blooms in coastal waters.

## 2. MATERIALS AND METHODS

### 2.1. Study area and sampling

The Sansha and Lianjiang areas are located in the coastal waters of Fujian Province in the East

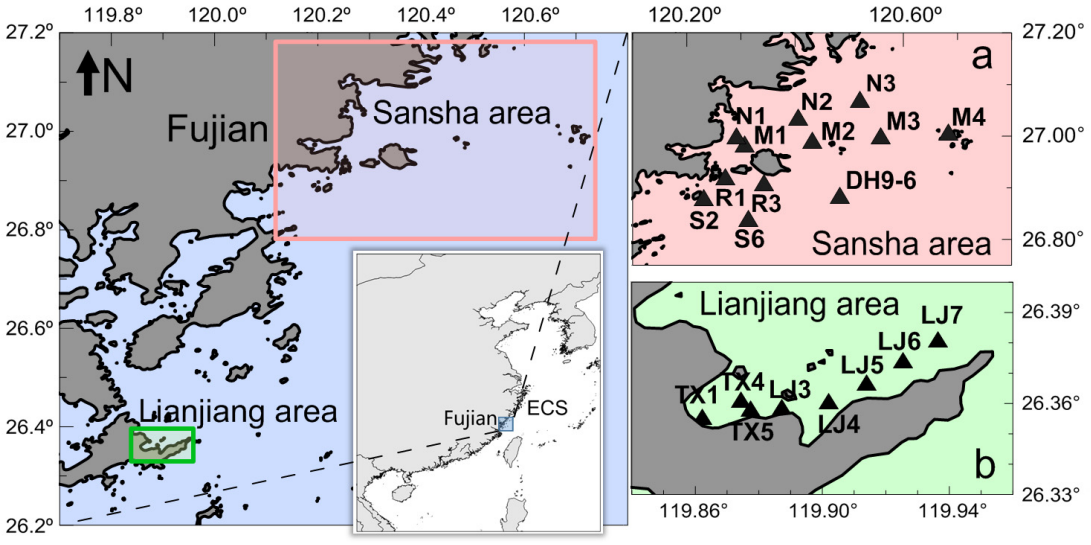


Fig. 1. Locations of sampling stations in the (a) Sansha and (b) Lianjian areas in the coastal waters of Fujian Province in the East China Sea (ECS)

China Sea (Fig. 1). Under the influence of human activities, especially mariculture, eutrophication has become a notable problem, and dinoflagellate blooms have occurred frequently in these waters during late spring and early summer in recent years (Li 2021, Niu et al. 2021). Three cruises were carried out on May 11–12, May 18–19, and May 24 2019 in the coastal waters of the Sansha area. During the first 2 cruises, a total of 12 stations were sampled (Fig. 1a). During the third cruise, only 7 stations (N1–3 and M1–4) were sampled. Another 3 cruises were carried out on May 20, May 25, and May 29 2019 in the coastal waters of the Lianjiang area. A total of 8 stations were sampled during each cruise (Fig. 1b).

Water samples were taken from the surface (0.5 m depth) using 2.5 l Niskin bottles. Hydrological data, cell densities of the dominant species, chl *a*, phosphorus nutrients, PMEA, and PDEA were measured at each station.

### 2.2. Determination of hydrological variables, chl *a* and cell density

A YSI 6600 V2 sonde was used to measure water temperature and salinity. The instrument was calibrated before cruises according to calibration procedures provided by the manufacturer.

Seawater samples of 150 ml were first filtered through a 200 µm filter to remove large zooplankton and then placed onto Whatman GF/F filters and stored at −20°C until analysis. The concentration of chl *a* was determined using a Trilogy Laboratory Fluorometer (Turner Designs) following extraction using 90% acetone in the dark for 24 h according to Parsons et al. (1984). Seawater samples of 1 l were mixed with 2% acid Lugol's solution and concentrated gradually to 20 ml prior to quantification. A 100 µl concentrated sample was transferred to a 0.1 ml counting chamber. Cells of the dominant species were quantified under a light microscope (Olympus CX31).

### 2.3. Phosphorus nutrient analyses

Seawater was filtered through precombusted (450°C, 2 h) GF/F filters and stored at −20°C until analysis. DIP concentration was determined using the molybdenum blue method described by Valderrama (1995), TDP concentration was analyzed according to the method of Jeffries et al. (1979), and DOP concentration was calculated by subtracting DIP from TDP.

The PMEase hydrolysable DOP ($DOP_{PME}$) and the PMEase and PDEase hydrolysable DOP ($DOP_{PME+PDE}$) were measured according to the method of Hashihama et al. (2013). Ten ml of filtered seawater was incubated with 100 µl of commercial PMEase (Sigma P7640) or a mixture of PMEase and PDEase (Worthington LS003926) and 100 µl of 0.5 mol $l^{-1}$ sodium azide in the dark for 4 h at 37°C. The final concentrations of PMEase and PDEase added were 1 and

0.04 unit ml$^{-1}$, respectively. $DOP_{PME}$ and $DOP_{PME+PDE}$ concentrations were calculated as the difference between DIP concentrations before and after the addition of the corresponding phosphatase/phosphatases. PDEase hydrolysable DOP ($DOP_{PDE}$) was calculated by subtracting the $DOP_{PME}$ from the $DOP_{PME+PDE}$. All phosphorus nutrient analyses were measured by a spectrophotometer (Hitachi U-4600) at 882 nm.

### 2.4. Phosphatase activity assays

Seawater was filtered through a 200 µm filter to remove large zooplankton. PMEA and PDEA were measured by monitoring the release of paranitrophenol from 1 mmol l$^{-1}$ paranitrophenylphosphate (Sigma P4744) and 1 mmol l$^{-1}$ bis-paranitrophenylphosphate (Sigma N3002), respectively, at 405 nm using a spectrophotometer (Yamaguchi et al. 2005). The seawater was filtered through 0.22 and 2 µm polycarbonate filters under <100 mm Hg of pressure, and thus the total PMEA and PDEA were divided into 3 size fractions: free-size (<0.22 µm), picosize (0.22–2 µm), and nano + microsize (2–200 µm). The subsamples were incubated in the dark at 30°C for 24 h. Sterilized seawater with substrates was used as the control, and calibration was performed with standard solutions of 4-nitrophenol spectrophotometric grade (Sigma 1048) in the range of 0.01–100 µmol l$^{-1}$.

### 2.5. Data analysis

All statistical analyses were performed with SPSS 21.0 software. A 1-way ANOVA was performed to compare parameters among the different cruises using Tukey's studentized range test (*t*-test), where a p-value of ≤0.05 was used to indicate the significance of the results. Prior to the analysis, data were tested for normality and homogeneity of variance. A $\log_{10}$ or square root transformation of the data was performed prior to any statistical test when necessary. Spearman correlation and multiple stepwise linear regression tests were applied to analyze the relationships between phosphatase activity and environmental variables (temperature, salinity, phosphorus nutrients, and phytoplankton biomass).

Table 1. Variation in temperature, salinity, chl *a*, and density of *Prorocentrum donghaiense* and *Karlodinium digitatum* (note the different unit multipliers) during the study periods. Data are mean ± SD. Cruises 1–3 were carried out May 11–12, May 18–19, and May 24 in 2019 in the Sansha area and May 20, May 25, and May 29 in 2019 in the Lianjiang area, respectively. A *P. donghaiense* bloom occurred in the Sansha area whereas a mixed bloom of *P. donghaiense* and *K. digitatum* occurred in the Lianjian area during the study periods. Superscript a, b and c indicate significant differences in variables among stations

| Variable | Cruise 1 | Cruise 2 | Cruise 3 |
|---|---|---|---|
| **Sansha** | | | |
| Temperature (°C) | 19.8 ± 0.6$^{a}$ | 22.7 ± 0.6$^{b}$ | 23.3 ± 1.0$^{b}$ |
| Salinity (‰) | 28.57 ± 0.96$^{a}$ | 27.98 ± 0.58$^{a}$ | 28.86 ± 0.79$^{a}$ |
| Chl *a* (µg l$^{-1}$) | 1.48 ± 0.48$^{a}$ | 13.51 ± 13.49$^{b}$ | 8.62 ± 12.12$^{a,b}$ |
| *P. donghaiense* density ($10^6$ cells l$^{-1}$) | 0.04 ± 0.03$^{a}$ | 11.74 ± 17.99$^{b}$ | 6.45 ± 11.14$^{a,b}$ |
| **Lianjiang** | | | |
| Temperature (°C) | 20.78 ± 0.31$^{a}$ | 21.90 ± 0.63$^{a}$ | 21.84 ± 0.15$^{a}$ |
| Salinity (‰) | 30.87 ± 0.13$^{a}$ | 31.00 ± 0.08$^{a}$ | 29.88 ± 2.03$^{a}$ |
| Chl *a* (µg l$^{-1}$) | 7.19 ± 6.23$^{a}$ | 14.00 ± 8.14$^{a,b}$ | 20.78 ± 7.56$^{b}$ |
| *P. donghaiense* density ($10^6$ cells l$^{-1}$) | 0.29 ± 0.21$^{a}$ | 4.88 ± 5.26$^{b}$ | 6.42 ± 4.25$^{c}$ |
| *K. digitatum* density ($10^5$ cells l$^{-1}$) | 3.39 ± 3.24$^{a}$ | 7.87 ± 9.55$^{a}$ | 6.68 ± 4.69$^{a}$ |

## 3. RESULTS

### 3.1. Hydrological variables, chl *a*, and cell densities

#### 3.1.1. Sansha area

During the study period of May 11 to 24 in 2019, seawater temperature varied from 19.0 to 25.2°C, and average temperature during the first cruise was significantly lower than during the second and third cruises ($p < 0.01$) (Table 1). Salinity ranged from 26.92 to 30.99, and average salinity did not differ among the 3 cruises ($p > 0.05$).

A dinoflagellate bloom caused by *P. donghaiense* occurred during the study period. During the first cruise, the density of *P. donghaiense* at most stations was lower than $5.0 \times 10^4$ cells l$^{-1}$ (Table 1). The highest *P. donghaiense* density, $1.35 \times 10^5$ cells l$^{-1}$, was observed at Stn S2. During the second cruise, patches of bloom were observed at Stns N3, M1, M2, M3, R3, and S6, with *P. donghaiense* densities varying from $1.44 \times 10^6$ to $5.60 \times 10^7$ cells l$^{-1}$. The average chl *a* increased significantly during the second cruise ($p < 0.05$), and during the third cruise, the bloom was sustained. The bloom center was observed at Stn M1, with a *P. donghaiense* density of $4.07 \times 10^7$ cells l$^{-1}$.

#### 3.1.2. Lianjiang area

During the study period of May 20 to 29 in 2019, seawater temperature and salinity ranged between 20.5 and 23.1°C and 26.17 and 31.75 respectively. Both average seawater temperature and salinity showed no difference among the three cruises ($p > 0.05$) (Table 1).

A mixed dinoflagellate bloom caused by *P. donghaiense* and *Karlodinium digitatum* was observed during the study period. During the first cruise, densities of both *P. donghaiense* and *K. digitatum* were ~$10^5$ cells $l^{-1}$. During the second cruise, *P. donghaiense* density at all stations except Stn TX1 was higher than $10^6$ cells $l^{-1}$. At the same time, *K. digitatum* density also increased at most stations. The highest densities of both *P. donghaiense* and *K. digitatum* were observed at Stn LJ4, at $1.71 \times 10^7$ and $2.94 \times 10^6$ cells $l^{-1}$ respectively. In addition, mass death of cultured fish was observed in the mariculture area close to Stn LJ4. During the third cruise, both *P. donghaiense* and *K. digitatum* remained at high densities. The average chl *a* during the third cruise was approximately 3 times that during the first cruise ($p < 0.01$).

### 3.2. Phosphorus nutrients

#### 3.2.1. Sansha area

Mean (±SD) DIP was 0.46 ± 0.12 µmol $l^{-1}$ during the first cruise; it decreased significantly to 0.11 ± 0.09 and 0.11 ± 0.05 µmol $l^{-1}$ during the second and third cruises respectively ($p < 0.01$) (Fig. 2a–c). DOP increased gradually from 0.60 ± 0.11 µmol $l^{-1}$ during the first cruise to 0.90 ± 0.31 µmol $l^{-1}$ during the third

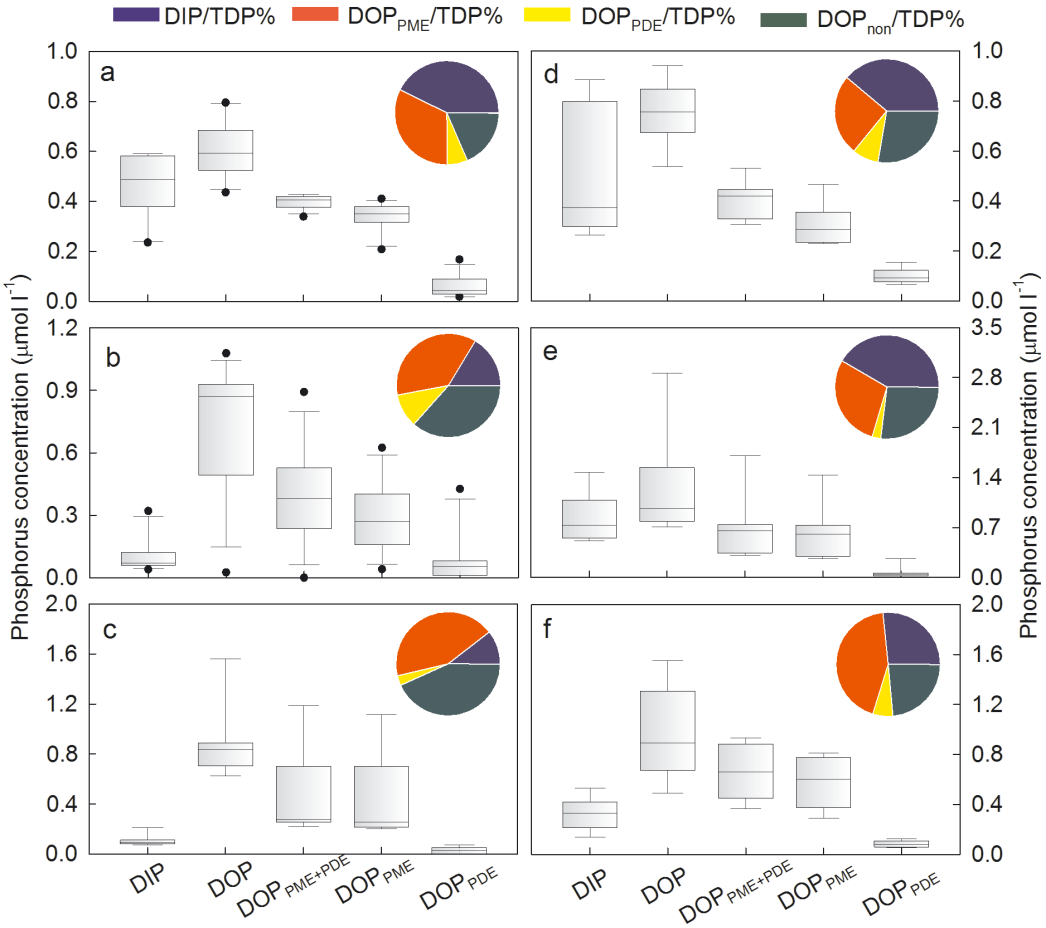


Fig. 2. Variation in the phosphorus concentrations in the (a–c) Sansha area and (d–f) Lianjang area during the (a,d) first, (b,e) second, and (c,f) third cruises (note the differences in y-axis scales). Boxes show concentrations of dissolved inorganic phosphorus (DIP), dissolved organic phosphorus (DOP), DOP hydrolysable by phosphomonoesterase (PMEase) and phosphodiesterase (PDEase) ($DOP_{PME+PDE}$), DOP hydrolysable by PMEase ($DOP_{PME}$), and DOP hydrolysable by PDEase ($DOP_{PDE}$). Horizontal line in box: median; top and bottom of box: Q3 and Q1 values; whiskers: upper and lower limits; dots: outliers. Pie charts show the contribution of DIP, $DOP_{PME}$, $DOP_{PDE}$, and nonhydrolysable DOP ($DOP_{non}$) to total dissolved phosphorus (TDP). DOP = $DOP_{PME}$ + $DOP_{PDE}$ + DOP-$_{non}$; TDP = DIP + DOP

cruise and showed a significant difference between the first and third cruises ($p < 0.05$). Average DOP was 1.4 times average DIP during the first cruise but increased greatly to 8.4–9.0 times average DIP during the second and third cruises. On average, DOP accounted for 57.4 ± 7.2, 83.6 ± 17.3, and 89.4 ± 2.0% of TDP during the first, second and third cruises, respectively.

Average $DOP_{PME+PDE}$ was 0.40 ± 0.03, 0.39 ± 0.22, and 0.49 ± 0.36 µmol $l^{-1}$ during the first, second, and third cruises, respectively, and accounted for more than 50% of DOP (Fig. 2a–c). Of this, $DOP_{PME}$ and $DOP_{PDE}$ contributed 77.3–93.9% and 6.1–22.7%, respectively, during the 3 cruises.

#### 3.2.2. Lianjiang area

During the entire study period, DIP was relatively high, with means (±SD) of 0.51 ± 0.26, 0.84 ± 0.33, and 0.33 ± 0.13 µmol $l^{-1}$ during the first, second, and third cruises, respectively (Fig. 2d–f). On average, DOP was 1.8 ± 0.8, 1.6 ± 0.9, and 3.8 ± 2.5 times DIP and accounted for 61.2 ± 12.8, 58.4 ± 13.1, and 73.4 ± 13.9% of TDP during the 3 cruises, respectively.

Average $DOP_{PME+PDE}$ varied from 0.31 to 1.70 µmol $l^{-1}$, and showed no difference among the 3 cruises ($p > 0.05$) (Fig. 2d–f). On average, $DOP_{PME+PDE}$ accounted for 54–69% of DOP during the 3 cruises. The average contribution of $DOP_{PME}$ to $DOP_{PME+PDE}$ was 75.0–90.7% during the 3 cruises.

### 3.3. Phosphatase activities

#### 3.3.1. Sansha area

PMEA was 0.07–0.51, 0.22–2.44, and 0.32–1.71 µmol $l^{-1}$ $h^{-1}$ during the first, second, and third cruises respectively (Fig. 3a–c). Average PMEA during the

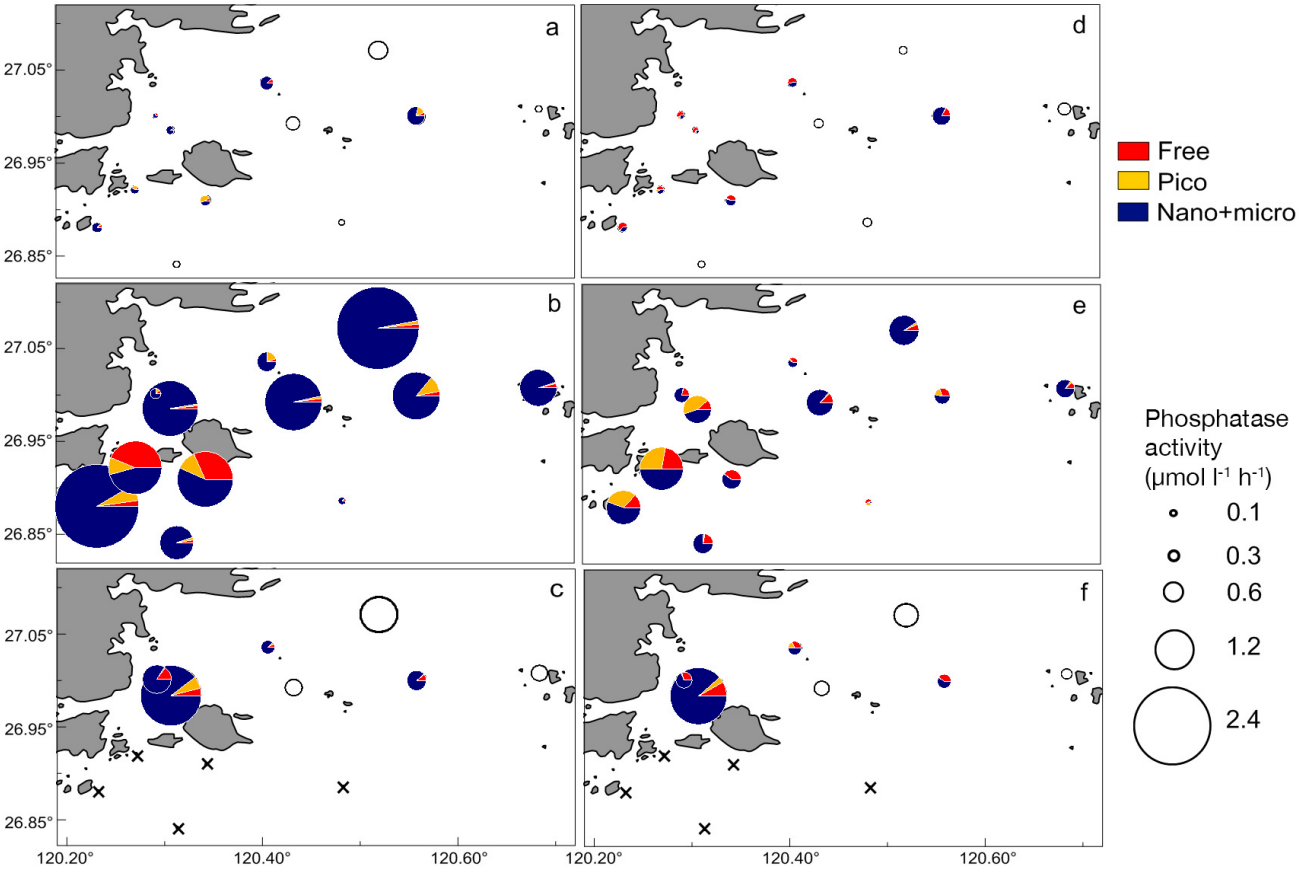


Fig. 3. Spatial distribution of (a–c) phosphomonoesterase (PMEase) activity (PMEA) and (d–f) phosphodiesterase (PDEase) activity (PDEA) in the Sansha area during the first (May 11–12), second (May 18–19), and third cruises (May 24) in 2019. The size of the circle shows the amount of total phosphatase activity. Total phosphatase is divided into nano + microsize (2–200 µm), picosize (0.22–2 µm), and free-size (<0.22 µm). During the first and third cruses, phosphatase activity was measured by size fraction at only some stations. Black circles: stations only measured with total phosphatase activities. × indicates stations where phosphatase activity was not measured during the third cruise

second cruise was approximately 5.4 times that during the first cruise ($p < 0.01$) and approximately 1.7 times that during the third cruise ($p > 0.05$) (Table 2). Average PDEA was significantly higher during the second and third cruises than during the first cruise ($p < 0.05$) (Fig. 3d–f, Table 2).

The average contribution of free-sized PMEA to total PMEA was approximately 10% during the 3 cruises. However, the average contribution of pico-sized PMEA to total PMEA decreased gradually, whereas the contribution of nano + microsized PMEA to total PMEA increased gradually (Table 2). The contribution of free-sized PDEA decreased from the first cruise to the third cruise, whereas that of nano + microsized PDEA increased (Table 2).

#### 3.3.2. Lianjiang area

Variations in PMEA and PDEA in the Lianjiang area were similar to those in the Sansha area during the 3 cruises (Fig. 4). Average PMEA and PDEA were higher during the second cruise but not significantly different from the first and third cruises ($p > 0.05$) (Table 2).

Throughout the entire study period, nano + microsized PMEA and PDEA accounted for 76.2–88.7% and 59.2–73.8% of total PMEA and PDEA, respectively, and free-sized PMEA and PDEA accounted for the next greatest proportion of PMEA and PDEA (Table 2).

### 3.4. Relationships between phosphatase activities and environmental variables

PMEA and PDEA were highly correlated in both study areas ($p < 0.01$), with the PMEA:PMEA ratio fixed at 2.5 (Fig. 5).

PMEA in both study areas showed positive correlations with chl *a*, cell density of the dominant species, and DOP ($p < 0.05$) (Fig. 6). In addition, in the Sansha area, PMEA was positively correlated with temperature ($p < 0.01$) and negatively correlated with DIP ($p < 0.05$), while in the Lianjiang area PMEA showed positive correlations with enzyme hydrolysable DOPs ($p < 0.05$).

PDEA in both study areas showed positive correlations with cell density of the dominant species, DOP, and enzyme hydrolysable DOP ($p < 0.05$) (Fig. 7). In the Sansha area, PDEA was positively correlated with DIP ($p < 0.05$), whereas in the Lianjiang area, PDEA was negatively correlated with DIP ($p < 0.05$). In addition, PDEA in the Lianjiang area showed positive correlations with temperature and chl *a* ($p < 0.05$).

In the Sansha area, chl *a* and temperature were the most important factors regulating PMEA and PEDA and explained 75.5 and 74.7% of their variation, respectively (Table 3). In the Lianjiang area, $DOP_{PME}$ and DOP were the most important factors regulating PMEA and PDEA and explained 50.3 and 62.3% of their variation, respectively.

## 4. DISCUSSION

### 4.1. Dinoflagellate blooms in the Sansha and Lianjiang areas

Due to anthropogenic activity, the coastal waters of Sansha and Lianjiang experience dinoflagellate blooms the most frequently of all areas in the East China Sea. Blooms of *Noctiluca scintillans, P. donghaiense*, *Karenia mikimotoi*, and *K. digitatum* have

Table 2. Variation in phosphomonoesterase (PMEase) activity (PMEA) and phosphodiesterase (PDEase) activity (PDEA) during the study periods. Cruises 1–3 were carried out on May 11–12, May 18–19, and May 24 in 2019 in the Sansha area and on May 20, May 25, and May 29 in 2019 in the Lianjiang area, respectively. Total phosphatase is divided into nano + microsize (2–200 µm), picosize (0.22–2 µm), and free-size (<0.22 µm). Superscripts letters indicate significant differences in variables among different stations

| Variable | Cruise 1 | Cruise 2 | Cruise 3 |
|---|---|---|---|
| **Sansha** | | | |
| Total PMEA (µmol $l^{-1}$ $h^{-1}$) | $0.24 \pm 0.14^{a}$ | $1.27 \pm 0.75^{b}$ | $0.75 \pm 0.50^{a,b}$ |
| Free (%) | 11.6 ± 7.1 | 10.0 ± 13.6 | 9.4 ± 4.6 |
| Pico (%) | 14.1 ± 17.0 | 6.8 ± 6.3 | 3.3 ± 2.8 |
| Nano + micro (%) | 74.3 ± 17.0 | 83.3 ± 16.9 | 87.4 ± 2.5 |
| Total PDEA (µmol $l^{-1}$ $h^{-1}$) | $0.21 \pm 0.09^{a}$ | $0.58 \pm 0.32^{b}$ | $0.56 \pm 0.48^{b}$ |
| Free (%) | 50.6 ± 17.4 | 23.5 ± 14.6 | 27.6 ± 13.7 |
| Pico (%) | 5.0 ± 5.2 | 14.5 ± 16.0 | 5.9 ± 7.9 |
| Nano + micro (%) | 44.5 ± 20.0 | 62.1 ± 23.2 | 66.5 ± 16.5 |
| **Lianjiang** | | | |
| Total PMEA (µmol $l^{-1}$ $h^{-1}$) | $0.54 \pm 0.23^{a}$ | $1.08 \pm 0.88^{a}$ | $0.87 \pm 0.61^{a}$ |
| Free (%) | 14.2 ± 10.6 | 12.6 ± 5.4 | 9.1 ± 6.7 |
| Pico (%) | 7.8 ± 3.4 | 11.3 ± 8.0 | 2.2 ± 4.3 |
| Nano + micro (%) | 78.1 ± 10.8 | 76.2 ± 4.0 | 88.7 ± 7.4 |
| Total PDEA (µmol $l^{-1}$ $h^{-1}$) | $0.59 \pm 0.20^{a}$ | $0.74 \pm 0.46^{a}$ | $0.52 \pm 0.23^{a}$ |
| Free (%) | 22.3 ± 6.6 | 25.9 ± 7.1 | 24.0 ± 12.6 |
| Pico (%) | 9.8 ± 16.4 | 14.9 ± 13.1 | 2.3 ± 3.1 |
| Nano + micro (%) | 67.9 ± 18.2 | 59.2 ± 11.9 | 73.8 ± 12.6 |

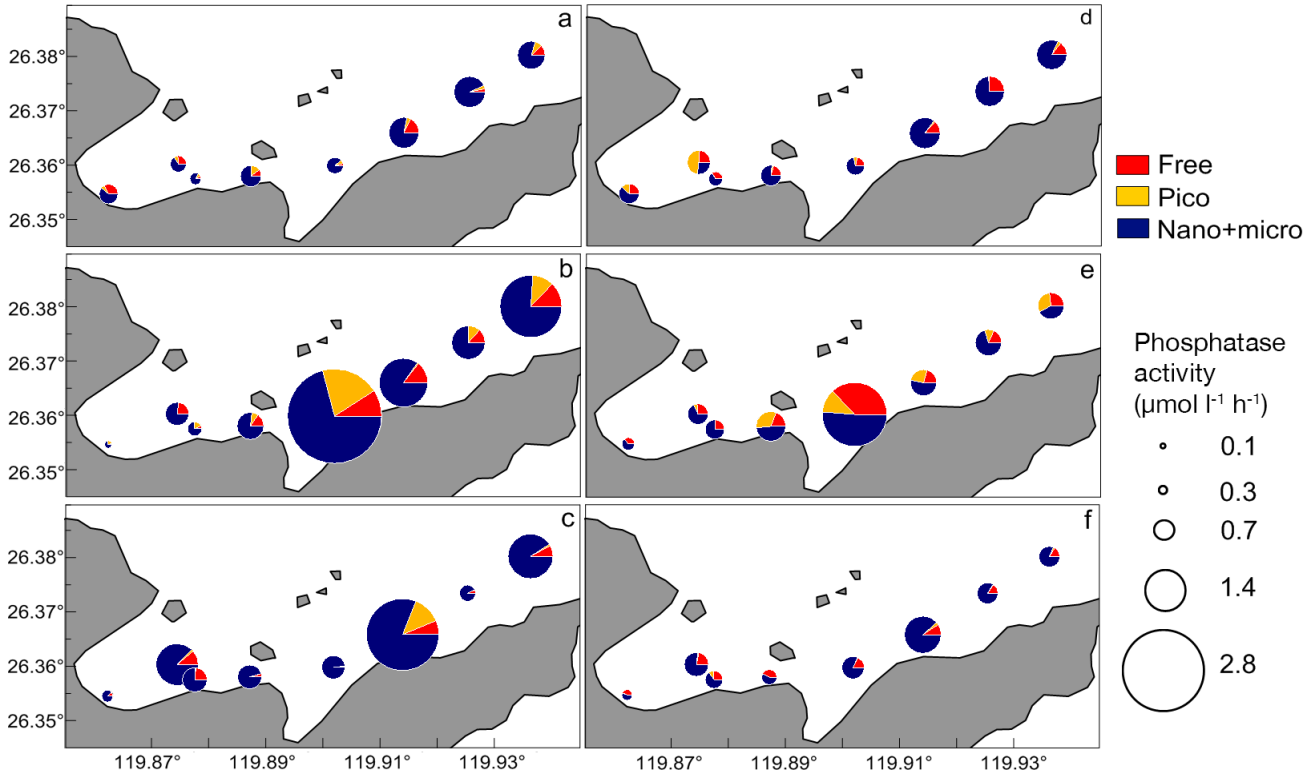


Fig. 4. Spatial distribution of (a–c) phosphomonoesterase (PMEase) activity (PMEA) and (d–f) phosphodiesterase (PDEase) activity (PDEA) in the Lianjiang area during the first (May 20), second (May 25), and third cruises (May 29) in 2019. The size of the circle shows the amount of total phosphatase activity. Total phosphatase is divided into nano + microsize (2–200 µm), picosize (0.22–2 µm), and free-size (<0.22 µm)

been reported in these areas, with *P. donghaiense* the most frequently occurring bloom species (Cen et al. 2020, Li 2021, Lu et al. 2022).

A density higher than $10^6$ cells $l^{-1}$ is considered the threshold of a *P. donghaiense* bloom (Lu & Goebel 2001). During the study period, the algal bloom in the Sansha area was caused by monospecies of *P. donghaiense*; the relatively low chl *a* and low *P. donghaiense* density during the first cruise suggested the incubation period of the bloom was occurring (Table 1). The bloom was observed during the second cruise and was maintained during the third cruise, although the biomass decreased to some degree (Table 1). Two possible reasons for the decrease in *P. donghaiense* density during the third cruise are limited phosphate in the seawater (Fig. 2c) and an increase in seawater temperature (Table 1). The optimum temperature for *P. donghaiense* blooms is 18 to 20°C; during the third cruise temperatures exceeded 23°C, which is not advantageous for the competitive growth of *P. donghaiense* in phytoplankton communities (Xu et al. 2010).

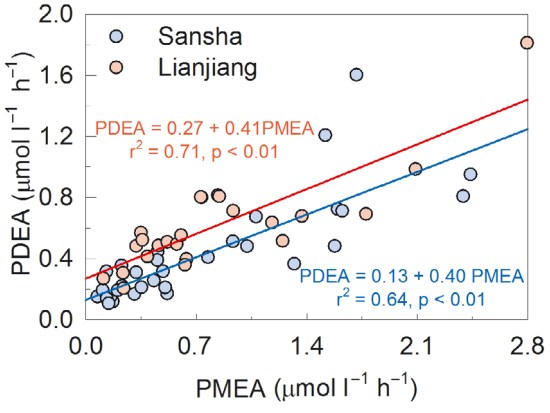


Fig. 5. Relationships between phosphomonoesterase (PMEase) activity (PMEA) and phosphodiesterase (PDEase) activity (PDEA) in the Sansha area (regression model in blue) and the Lianjiang area (regression model in red)

The *P. donghaiense* bloom in the Lianjiang area was accompanied by a *K. digitatum* bloom. In contrast to nontoxic *P. donghaiense* blooms (Lu et al. 2022), *K. digitatum* blooms have often been correlated with fish kills (Cen et al. 2020, Sakamoto et al. 2021). The pre-bloom period occurred during the first cruise in this area, and both *P. donghaiense* and *K. digitatum* cell densities reached $10^5$ cells $l^{-1}$

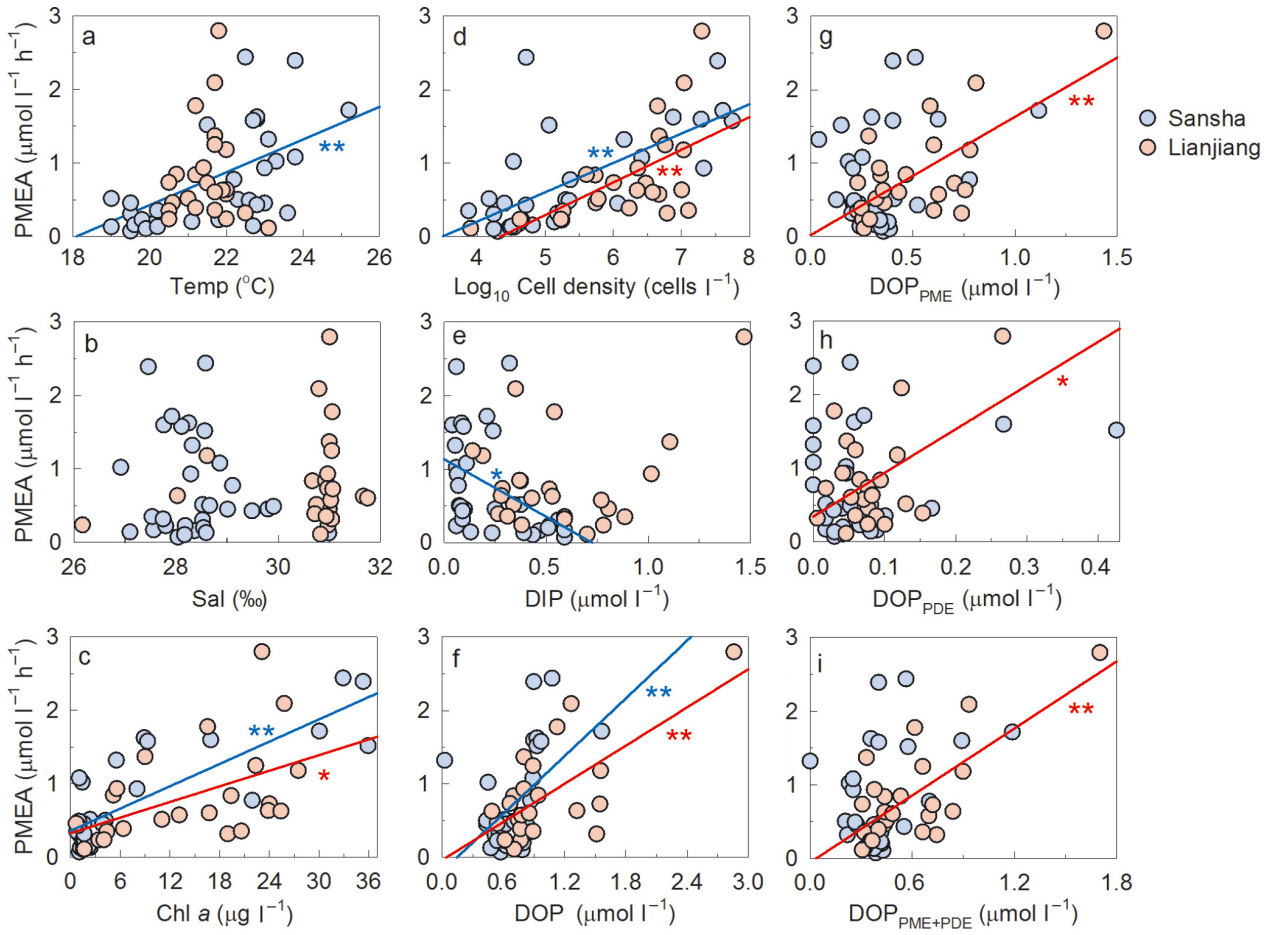


Fig. 6. Variation in phosphomonoesterase (PMEase) activity (PMEA) with (a) temperature ($T$), (b) salinity (Sal), (c) chl *a*, (d) cell density, (e) dissolved inorganic phosphorus (DIP), (f) dissolved organic phosphorus (DOP), (g) DOP hydrolysable by PMEase ($DOP_{PME}$), (h) DOP hydrolysable by phosphodiesterase (PDEase) ($DOP_{PDE}$), and (i) DOP hydrolysable by PMEase and PDEase ($DOP_{PME+PDE}$) in the Sansha and Lianjiang areas during the study period. Cell density in the Sansha area indicates the density of *Prorocentrum donghaiense*, whereas cell density in the Lianjiang area includes the densities of both *P. donghaiense* and *Karlodinium digitatum.* Blue and red lines show regressions for each area and asterisks indicate significant relationships between PMEA and the independent variable. $^{*}p < 0.05$; $^{**}p < 0.01$

(Table 1). During the second cruise, *P. donghaiense* maintained this bloom density (Table 1), while *K. digitatum* doubled in density. In addition, a large fish kill was observed in the study area (Table 1); thus, it was concluded that a bloom of *K. digitatum* also occurred. As environmental conditions remained suitable between the second and third cruises, the blooms reached an even higher biomass during the third cruise (Table 1).

### 4.2. Different external phosphorus conditions in the two dinoflagellate bloom areas

Due to the unbalanced input of nitrogen and phosphorus into seawater, the coastal waters of the East China Sea have higher N:P ratios than the Redfield ratio of 16:1 (Redfield 1958) and are potentially phosphorus limited (Liu et al. 2016). The importance of DOP as the major phosphorus source during *P. donghaiense* blooms has been suggested in several studies (Huang et al. 2007, Ou et al. 2008, 2020, Zhou et al. 2019). In the Sansha area, DIP decreased rapidly with the rapid growth of *P. donghaiense* to the phosphate limitation threshold of 0.1 μmol l$^{-1}$ (Justíc et al. 1995) (Fig. 2a–c). In contrast, DOP increased (Fig. 2b–c), which might have been due to the abundant organic metabolic products released into the seawater by bloom-causing species (Lin et al. 2016, Zhou et al. 2019). In addition, DOP, which accounted for more than 80% of TDP, became the most important phosphorus source for maintenance of the *P. donghaiense* bloom (Fig. 2b–c). The DOP pool can be divided into labile DOP and stable DOP, depending on whether

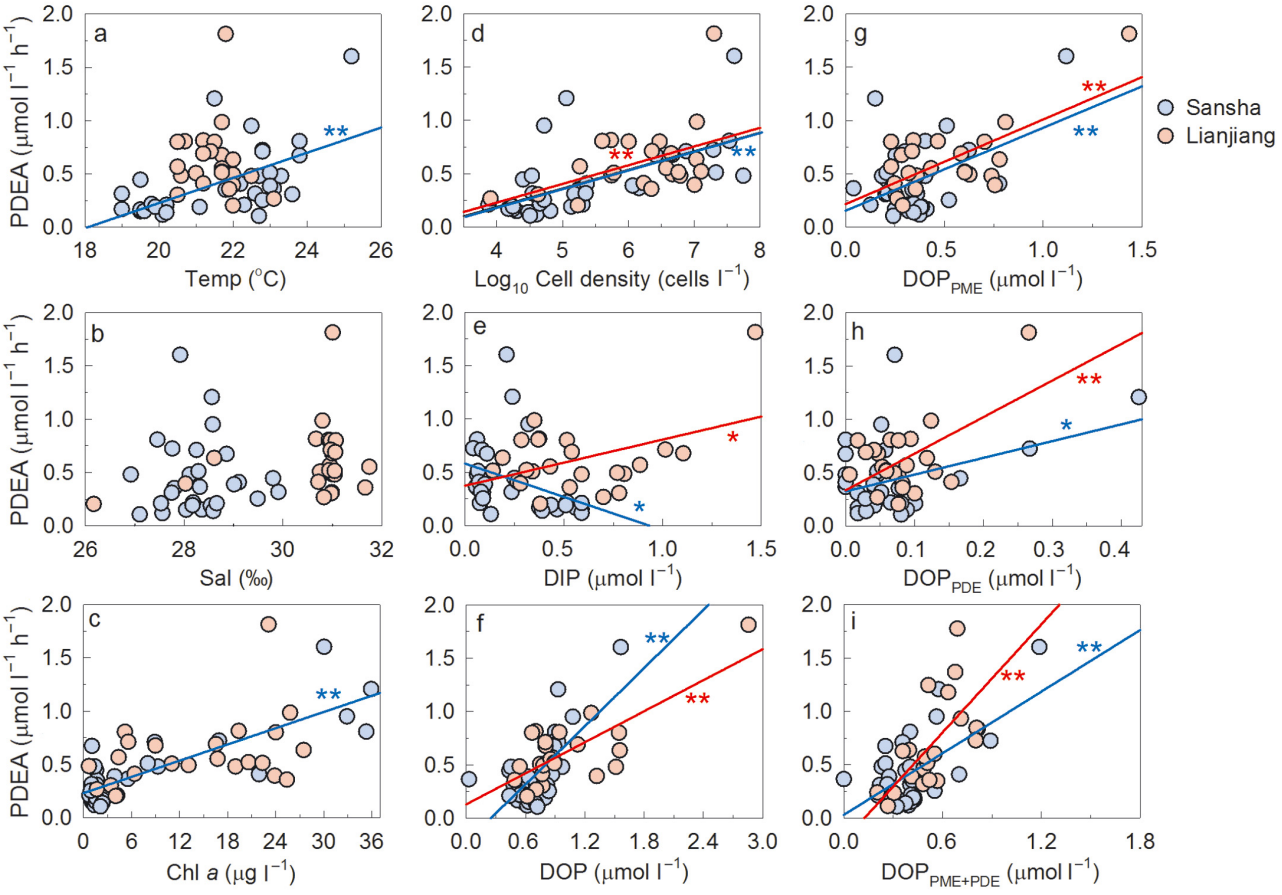


Fig. 7. Variations in phosphodiesterase (PDEase) activity (PDEA) with (a) temperature ($T$), (b) salinity (Sal), (c) chl *a*, (d) cell density, (e) dissolved inorganic phosphorus (DIP), (f) dissolved organic phosphorus (DOP), (g) DOP hydrolysable by phosphomonoesterase (PMEase) ($DOP_{PME}$), (h) DOP hydrolysable by PDEase ($DOP_{PDE}$), and (i) DOP hydrolysable by PMEase and PDEase ($DOP_{PME+PDE}$) in the Sansha and Lianjiang areas during the study period. Cell density in the Sansha area indicates the density of *Prorocentrum donghaiense*, whereas cell density in the Lianjiang area includes the densities of both *P. donghaiense* and *Karlodinium digitatum.* Blue and red lines show regressions for each area and asterisks indicate significant relationships between PDEA and the independent variable. *$p < 0.05$; **$p < 0.01$

the phosphorus is easily hydrolyzed by microorganisms (Karl & Yanagi 1997, Kolowith et al. 2001). Labile organic phosphorus accounts for 68% of DOP in estuaries, and high values normally occur in summer and autumn with high amounts of biomass (Monbet et al. 2009). The present results showed that labile DOP ($DOP_{PME+PDE}$) accounted for more than 50% of DOP and was 3–4 times the amount of DIP (Fig. 2b–c), which further emphasized the importance of DOP regeneration during the bloom when phosphate was depleted.

Coastal environments with DIP higher than 0.3 μmol $l^{-1}$ are considered phosphate-rich (Labry et al. 2016). Thus, in contrast to the phosphate

Table 3. Stepwise linear regression analysis of phosphomonoesterase (PMEase) activity (PMEA) and phosphodiesterase (PDEase) activity (PDEA) with environmental variables in the coastal waters of the Sansha and Lianjiang areas. The dependent variable was PMEA or PDEA; independent variables were temperature ($T$), salinity, dissolved inorganic phosphorus (DIP), dissolved organic phosphorus (DOP), DOP hydrolysable by PMEase ($DOP_{PME}$), DOP hydrolysable by PDEase ($DOP_{PDE}$), density of bloom-causing species (*Prorocentrum donghaiense* in Sansha, or *P. donghaiense* and *Karlodinium digitatum* in Lianjiang), and chl *a*. The regression was set to reject any variable that failed to produce an $F$ statistic significant at the p = 0.05 level

| Dependent variable | Model | $r^2$ | p |
|---|---|---|---|
| **Sansha** | | | |
| PMEA | PMEA = −2.399 + 0.042chl *a* + 0.130$T$ | 0.755 | < 0.001 |
| PDEA | PDEA = −0.971 + 0.022chl *a* + 0.057$T$ | 0.747 | < 0.001 |
| **Lianjiang** | | | |
| PMEA | PMEA = −0.097 + 1.563$DOP_{PME}$ | 0.503 | < 0.001 |
| PDEA | PDEA = 0.095 + 0.086DOP | 0.623 | < 0.001 |

deficiency in the Sansha area, blooms in the Lianjiang area occurred under phosphate-replete conditions during the surveys (Fig. 2d–f). DOP concentrations also increased, and the contribution of DOP to TDP increased from ~60 to ~70% during the bloom (Fig. 2d–f). In contrast to the $DOP_{PME+PDE}$/DOP ratio in the Sansha area, which decreased from 68 to ~50%, suggesting labile DOP was hydrolyzed during the bloom when phosphate was scarce, the $DOP_{PME+PDE}$/DOP ratio in the Lianjiang area increased from 54 to 69%, suggesting labile DOP accumulated during the bloom when phosphate was abundant (Fig. 2a–f). Hence, DOP might also have become important to the development of the bloom when phosphate was exhausted in the Lianjiang area.

Concentrations of PDE are normally considered to be much lower than those of PME in seawater, and are less studied (Benitez-Nelson 2000, Sato et al. 2013). However, the limited studies available show concentrations of PDE are comparable with those of PME in some coastal waters, and emphasize the importance of PDE as an available phosphorus source (Suzumura et al. 1998, Monbet et al. 2009). The concentration of PDE is normally lower than 40 nmol $l^{-1}$ in open oceans, but may be as high as 230 nmol $l^{-1}$ in some coastal areas (Yamaguchi et al. 2021). In the present study, during both blooms, $DOP_{PDE}$ concentrations ranged from undetectable to 0.47 µmol $l^{-1}$. $DOP_{PME}$ accounted for 75 to 94% of labile DOP, whereas $DOP_{PDE}$ accounted for 6 to 25% of labile DOP (Fig. 2), suggesting that PME was the most abundant phosphate ester available during the blooms. The several-fold increase in $DOP_{PME}$ within the Lianjiang bloom area during the bloom period (Fig. 2d–f) also suggested that PME was the main metabolic organic phosphorus product released by phytoplankton.

### 4.3. PMEA, PDEA, and their regulation

Many studies have been done on PMEA and its regulation (Sebastián et al. 2004, Huang et al. 2007, Labry et al. 2016, Davis & Mahaffey 2017, Mo et al. 2020, Srivastava et al. 2021, Lidbury et al. 2022). These studies have shown that PMEA might be affected by environmental variables, such as external phosphate and DOP availability, temperature, salinity, pH, and UV radiation (Hoppe 2003). The physiological status of microorganisms and their different responses to PMEase might also influence PMEA (Hoppe 2003, Dyhrman 2016, Ou et al. 2020). In addition to the canonical PMEases (PhoA, PhoD, and PhoX), which are sensitive to external phosphate and are inducible by microorganisms under phosphorus stress conditions, Lidbury et al. (2021, 2022) reported a phosphate-insensitive and constitutive PMEase, termed PafA. Different PMEase families have different regulatory mechanisms (Lidbury et al. 2022).

To date, the regulation of PDEA is largely unknown (Thomson et al. 2020). Sato et al. (2013) suggested that PDEA is regulated more by phosphate availability than by DOP in the Pacific Ocean, while Yamaguchi et al. (2021) observed that the distribution of PDEA is independent of phosphate, PME, or DOP concentrations in a subtropical oligotrophic ocean, indicating more complex regulation of PDEA than of PMEA. The present study demonstrated that regulation of PMEA and PDEA showed some similarities, both increasing with temperature and phytoplankton biomass (chl *a* and cell density) (Figs. 6 & 7). Both PMEA and PDEA were upregulated when phosphate was depleted, and both increased with external DOP concentrations under both phosphate-depleted and phosphate-replete conditions (Figs. 6 & 7). PDEA hydrolyzes PDE to PME, which can be further hydrolyzed by PMEA (Sato et al. 2013, Yamaguchi et al. 2020), suggesting the regulation of PMEA might be more sensitive to external phosphate availability, whereas the regulation of PDEA might be more sensitive to external DOP availability.

In this study, only phytoplankton biomass and the dominant algal species were considered; information about bacterial biomass and community structure was lacking. Bacteria are major producers of phosphatases (Hoppe 2003, Dyhrman 2016). During blooms, the nano + microsized PMEA and PDEA accounted for most of the total phosphatase activity (Table 2), which suggested that bloom-causing species and/or bacteria attached to the cells were the major phosphatase producers. This finding is consistent with those of previous studies conducted during blooms (Huang et al. 2007, Ou et al. 2018), and in some non-axenic monoculture laboratory studies (Ellwood et al. 2020). Some major bacterial phosphatase producers, such as Bacteroidetes, frequently associate with phytoplankton and sinking particles (Lidbury et al. 2021, 2022). Given that different bacterial taxa produce different families of phosphatases (PhoA, PhoD, PhoX, and PafA) (Lidbury et al. 2022), a study of coexisting bacterial taxonomy or a direct analysis of phosphatase families and their dynamic patterns might help clarify the regulation of phosphatases during blooms.

The present results showed that PMEA and PDEA were highly correlated. Regardless of the external phosphate conditions, PDEA was always approxi-

mately 40% of PMEA (Fig. 5). These results suggested potential expression differences between the 2 phosphatases, as PMEase and PDEase play different roles in the hydrolysis of different DOP groups (Cembella et al. 1982). Higher PMEase relative to PDEase in seawater normally indicates a higher content of PME to be hydrolyzed (Sato et al. 2013). In epiphytic mats produced by the dinoflagellate *Ostreopsis ovata* on the Mediterranean coast, a PMEA:PDEA ratio of 1.3 was observed (Accoroni et al. 2017). However, in some ocean waters, PMEA has been observed to be several times greater than PDEA (Sato et al. 2013, Thomson et al. 2020). A lower ratio of PMEA:PDEA in coastal waters might reflect more abundant PDE in coastal waters than in oceanic waters. However, it is worth noting that compared with PMEase, which is generally promiscuous, PDEase is more substrate-specific and might not react with the PDE substrate of bis-paranitrophenylphosphate used in this study (Srivastava et al. 2021); thus, PDEA might be underestimated.

In the Sansha area, both PMEA and PDEA increased significantly from the first to the second cruise and maintained high values during the third cruise (Fig. 3, Table 2). In the Lianjiang area, phosphatase activity increased slightly during the second cruise but did not differ significantly from the other cruises (Fig. 4, Table 2). PMEase and PDEase are inducible enzymes under phosphate deficiency (Cembella et al. 1982, Dyhrman 2016, Huang et al. 2021), and the contrasting external phosphate conditions during the 2 blooms were important in determining variation in temporal trends in phosphatase activity in the Sansha and Lianjiang areas.

Furthermore, different bloom stages during the surveys in the Sansha and Lianjiang areas could explain why the sites differed in phosphatase activity levels. The investigation in the Sansha area started during the bloom incubation period and continued into the bloom period, whereas the investigation in the Lianjiang area started during the pre-bloom period. Thus, algal bloom biomasses were significantly different between the 2 areas. During the bloom period of the second cruise in both areas, when the biomass of chl *a* was similar, the predicted higher phosphatase activity in the phosphate-depleted Sansha area relative to the phosphate-replete Lianjiang area was not observed. Rather, phosphatase activities in the 2 areas were comparable (Table 1). Qin et al. (2021) also observed high PMEA during a *P. donghaiense* bloom in a phosphate-replete environment and suggested that PMEA was regulated by cellular growth demand for phosphorus rather than the external phosphorus availability. Rapid growth might have induced bloom-causing species to express abundant phosphatases in the Lianjiang area even when phosphate was abundant. Lidbury et al. (2022) reported a previously overlooked but abundant constitutive PMEase of PafA that is prevalent in Bacteroidetes. Bacteroidetes normally bloom alongside phytoplankton, and typically associate with phytoplankton and sinking particles. The high proportion of PMEA and PDEA attached to particles during blooms, whether in phosphate-replete or phosphate-depleted conditions, might be partially attributed to Bacteriodietes. Microorganisms have shown differences in phosphatase characteristics, including amount of phosphatase production (Ou et al. 2010, 2020, Dyhrman 2016) and phosphatase families (Lidbury et al. 2022). Thus, different microbial community structures in the 2 study areas might also affect phosphatase activities.

## 5. CONCLUSIONS

The present study showed *P. donghaiense* blooms may occur under both phosphate-depleted and phosphate-replete conditions. Regardless of the external phosphate conditions, DOP was an important phosphorus source during the blooms. More than 50% of DOP was labile, and the availability of DOP sustained the blooms, especially when phosphate was depleted. PMEase and PDEase were abundantly expressed during the blooms to utilize the different groups of DOP, with PMEA and PDEA being highly correlated and their regulation showing some similarity. Both PMEA and PDEA increased with the decrease in DIP when phosphate was depleted but increased with DOP regardless of the external phosphate conditions. Temperature and biomass were the crucial variables regulating both PMEase and PDEase during bloom under phosphate-depleted conditions, whereas the availability of DOP was the crucial variable regulating both PMEase and PDEase during bloom under phosphate-replete conditions. The present study showed the important role of DOP recycling during dinoflagellate blooms, and suggested the regulation of PMEase and PDEase by environmental variables was similar during both blooms, although the most crucial variables might change depending on external phosphate conditions.

*Acknowledgements.* The authors would like to thank 3 anonymous reviewers for their constructive comments on the manuscript. This work was supported by the National Science Foundation of China (grant numbers 42176201 and 41776121).

LITERATURE CITED


Accoroni S, Totti C, Razza E, Congestri R, Campanelli A, Marini M, Ellwood NTW (2017) Phosphatase activities of a microepiphytic community during a bloom of *Ostreopsis* cf. *ovata* in the northern Adriatic Sea. Water Res 120: 272–279

Benitez-Nelson CR (2000) The biogeochemical cycling of phosphorus in marine systems. Earth Sci Rev 51:109–135

Björkman KM (2014) Polyphosphate goes from pedestrian to prominent in the marine P-cycle. Proc Natl Acad Sci USA 111:7890–7891

Cembella AD, Antia NJ, Harrison PJ (1982) The utilization of inorganic and organic phosphorous compounds as nutrients by eukaryotic microalgae: a multidisciplinary perspective. I. CRC Crit Rev Microbiol 10:317–391

Cen JY, Wang JY, Huang LF, Ding GM and others (2020) Who is the 'murderer' of the bloom in coastal waters of Fujian, China, in 2019? J Oceanol Limnol 38:722–732

Davis CE, Mahaffey C (2017) Elevated alkaline phosphatase activity in a phosphate-replete environment: influence of sinking particles. Limnol Oceanogr 62:2389–2403

Duhamel M, Arítegui J, Montero MF, Escanez J, Niell FX (2004) Alkaline phosphatase activity and its relationship to inorganic phosphorus in the transition zone of the North-western African upwelling system. Prog Oceanogr 62:131–150

Duhamel S, Dyhran ST, Karl DM (2010) Alkaline phosphatase activity and regulation in the North Pacific Subtropical Gyre. Limnol Oceanogr 55:1414–1425

Dyhrman ST (2016) Nutrients and their acquisition: phosphorus physiology in microalgae. In: Borowitzka MA, Beardall J, Raven JA (eds) The physiology of microalgae. Springer, Berlin, p 159–187

Ellwood NTW, Pasella MM, Totti C, Accoroni S (2020) Growth and phosphatase activities of *Ostreopsis* cf. *ovata* biofilms supplied with diverse dissolved organic phosphorus (DOP) compounds. Aquat Microb Ecol 85: 155–166

Ghyoot C, Gypens N, Flynn KJ, Lancelot C (2015) Modelling alkaline phosphatase activity in microalgae under orthophosphate limitation: the case of *Phaeocystis globosa*. J Plankton Res 37:869–885

Harrison PJ, Hu MH, Yang YP, Lu X (1990) Phosphate limitation in estuarine and coastal waters of China. J Exp Mar Biol Ecol 140:79–87

Hashihama F, Kinouchi S, Suwa S, Suzumura M, Kanda J (2013) Sensitive determination of enzymatically labile dissolved organic phosphorus and its vertical profiles in the oligotrophic western North Pacific and East China Sea. J Oceanogr 69:357–367

Hoppe HG (2003) Phosphatase activity in the sea. Hydrobiologia 493:187–200

Huang BQ, Ou LJ, Wang XL, Huo WY and others (2007) Alkaline phosphatase activity of phytoplankton in East China Sea coastal waters with frequent harmful algal bloom occurrences. Aquat Microb Ecol 49:195–206

Huang KX, Zhuang YQ, Wang Z, Ou LJ, Cen JY, Lu SH, Qi YZ (2021) Bioavailability of organic phosphorus compounds to the harmful dinoflagellate *Karenia mikimotoi*. Microorganisms 9:1961

Jeffries DS, Dieken FP, Jones DE (1979) Performance of the autoclave digestion method for total phosphorus analysis. Water Res 13:275–279

Justíc D, Rabalais NN, Turner RE, Dortch Q (1995) Changes in nutrient structure of river-dominated coastal waters: stoichiometric nutrient balance and its consequences. Esutar Coast Shelf Sci 40:339–356

Karl DM (2014) Microbially mediated transformations of phosphorus in the sea: new views of an old cycle. Annu Rev Mar Sci 6:279–337

Karl DM, Yanagi K (1997) Partial characterization of the dissolved organic phosphorus pool in the oligotrophic North Pacific Ocean. Limnol Oceanogr 42:1398–1405

Kolowith LC, Ingall ED, Benner R (2001) Composition and cycling of marine organic phosphorus. Limnol Oceanogr 46:309–320

Labry C, Delmas D, Youenou A, Quere J and others (2016) High alkaline phosphatase activity in phosphate replete waters: the case of two macrotidal estuaries. Limnol Oceanogr 61:1513–1529

Li X (2021) The influence of SST on the red tide near Huangqi in Lianjiang. Mar Forecast 38:95–103 (in Chinese with English abstract)

Li Y, Lu SH, Jiang TJ, Xiao YP, You SP (2011) Environmental factors and seasonal dynamics of *Prorocentrum* populations in Nanji Islands National Nature Reserve, East China Sea. Harmful Algae 10:426–432

Lidbury IDEA, Borsetto C, Murphy ARJ, Bottrill A and others (2021) Niche-adaptation in plant-associated Bacteroidetes favours specialization in organic phosphorus mineralization. ISME J 15:1040–1055

Lidbury IDEA, Scanlan DJ, Murphy ARJ, Christie-Oleza JA, Augilo-Ferretjans MM, Hitchcock A, Daniell TJ (2022) A widely distributed phosphate-insensitive phosphatase presents a route for rapid organophosphorus remineralization in the biosphere. Proc Natl Acad Sci USA 119: e2118122119

Lin SJ, Litaker RW, Sunda WG (2016) Phosphorus physiological ecology and molecular mechanisms in marine phytoplankton. J Phycol 52:10–36

Liu SM, Qi XH, Li XN, Ye HR and others (2016) Nutrient dynamics from the Changjiang (Yangtze River) estuary to the East China Sea. J Mar Syst 154:15–27

Lomas MW, Burke ML, Lomas DA, Bell DW, Shen C, Dyhrman ST, Ammerman JW (2010) Sargasso Sea phosphorus biogeochemistry: an important role for dissolved organic phosphorus (DOP). Biogeosciences 7: 695–710

Lu DD, Goebel J (2001) Five red tide species in genus *Prorocentrum* including the description of *Prorocentrum donghaiense* Lu sp. nov. from the East China Sea. Chin J Oceanol Limnol 19:337–344

Lu SH, Ou LJ, Dai XF, Cui L and others (2022) An overview of *Prorocentrum donghaiense* blooms in China: species identification, occurrences, ecological consequences, and factors regulating prevalence. Harmful Algae 114: 102207

Malone TC, Newton A (2020) The globalization of cultural eutrophication in the coastal ocean: causes and consequences. Front Mar Sci 7:670

Martin P, Lauro FM, Sarkar A, Goodkin N, Prakash S, Vinayachandran PN (2018) Particulate polyphosphate and alkaline phosphatase activity across a latitudinal transect in the tropical Indian Ocean. Limnol Oceanogr 63:1395–1406

Mills MM, Ridame C, Davey M, La Roche J, Geider RJ (2004) Iron and phosphorus co-limited nitrogen fixation in the eastern tropical North Atlantic. Nature 429: 292–294

Mo Y, Ou LJ, Lin LZ, Huang BQ (2020) Temporal and spatial variations of alkaline phosphatase activity related to phosphorus status of phytoplankton in the East China Sea. Sci Total Environ 731:139192

Monbet P, McKelvie ID, Worsfold PJ (2009) Dissolved organic phosphorus speciation in the waters of the Tamar estuary (SW England). Geochim Cosmochim Acta 73:1027–1038

Niu SJ, Li MT, Tong M, Liu XQ, Liu MD, Yin GY (2021) Response of distribution of water quality in the Sansha Bay on the land discharge and aquaculture. Haiyang Huanjiang Kexue 40:41–49

Ou LJ, Wang D, Huang BQ, Hong HS, Qi YZ, Lu SH (2008) Comparative study on phosphorus strategies of three typical harmful algae in Chinese coastal waters. J Plankton Res 30:1007–1017

Ou LJ, Huang BQ, Hong HS, Qi YZ, Lu SH (2010) Comparative alkaline phosphatase characteristics of the algal bloom species *Prorocentrum donghaiense, Alexandrium catenella* and *Skeletonema costatum.* J Phycol 46: 260–265

Ou LJ, Liu XH, Li JJ, Qin XL, Cui L, Lu SH (2018) Significant activities of extracellular enzymes from a brown tide in the coastal waters of Qinhuangdao, China. Harmful Algae 74:1–9

Ou LJ, Qin XL, Shi XY, Feng QL, Zhang SW, Lu SH, Qi YZ (2020) Alkaline phosphatase activities and regulation in three harmful *Prorocentrum* species from the coastal waters of East China Sea. Microb Ecol 79:459–471

Parsons TR, Yoshiaki M, Lalli CM (1984) A manual of chemical and biological methods for seawater analysis. Pergamon Press, Oxford

Qin XL, Shi XY, Gao YH, Ou LJ and others (2021) Alkaline phosphatase activity during a phosphate replete dinoflagellate bloom caused by *Prorocentrum obtusidens.* Harmful Algae 103:101979

Redfield AC (1958) The biological control of chemical factors in the environment. Am Sci 46:205–222

Reinhard CT, Planavsky NJ, Gill BC, Ozaki K and others (2016) Evolution of the global phosphorus cycle. Nature 541:386–389

Sakamoto S, Lim WA, Lu DD, Dai XF, Orlova T, Iwataki M (2021) Harmful algal blooms and associated fisheries damage in East Asia: current status and trends in China, Japan, Korea and Russia. Harmful Algae 102:101787

Sato M, Sakuraba R, Hashihama F (2013) Phosphate monoesterase and diesterase activities in the North and South Pacific Ocean. Biogeosciences 10:7677–7688

Sebastián M, Arítegui J, Montero MF, Escanez J, Niell FX (2004) Alkaline phosphatase activity and its relationship to inorganic phosphorus in the transition zone of the north-western African upwelling system. Prog Oceanogr 62:131–150

Srivastava A, Saavedra DM, Thomson B, García JAL and others (2021) Enzyme promiscuity in natural environments: alkaline phosphatase in the ocean. ISME J 15: 3375–3383

Suzumura M, Ingall ED (2004) Distribution and dynamics of various forms of phosphorus in seawater: insights from field observations in the Pacific Ocean and a laboratory experiment. Deep Sea Res I 51:1113–1130

Suzumura M, Ishikawa K, Ogawa H (1998) Characterization of dissolved organic phosphorus in coastal seawater using ultrafiltration and phosphohydrolytic enzymes. Limnol Oceanogr 43:1553–1564

Thomson B, Wenley J, Lockwood S, Twigg I and others (2020) Relative importance of phosphodiesterase vs. phosphomonoesterase (alkaline phosphatase) activities for dissolved organic phosphorus hydrolysis in epi- and mesopelagic waters. Front Earth Sci 8:560893

Valderrama JC (1995) Methods of nutrient analysis. In: Hallegraeff GM, Anderson DM, Cembella AD (eds) Manual on harmful marine microalgae. UNESCO Publishing, Paris, p 251–568

Xu N, Duan SS, Li AF, Zhang CW, Cai ZP, Hu ZX (2010) Effect of temperature, salinity and irradiance on the growth of the harmful dinoflagellate *Prorocentrum donghaiense* Lu. Harmful Algae 9:13–17

Yamaguchi H, Yamaguchi M, Fukami K, Adachi M, Nishijima T (2005) Utilization of phosphate diester by the marine diatom *Chaetoceros ceratosporus.* J Plankton Res 27: 603–606

Yamaguchi H, Arisaka H, Otsuka N, Tomaru Y (2014) Utilization of phosphate diesters by phosphodiesterase-producing marine diatoms. J Plankton Res 36:281–285

Yamaguchi T, Sato M, Hashihama F, Ehama M, Shiozaki T, Takahashi K, Furuya K (2019) Basin-scale variations in labile dissolved phosphoric monoesters and diesters in the central North Pacific Ocean. J Geophys Res Oceans 124:3058–3072

Yamaguchi T, Sato M, Gonda N, Takahashi K, Furuya K (2020) Phosphate diester utilization by marine diazotrophs *Trichodesmium erythraeum* and *Crocosphaera watsonii.* Aquat Microb Ecol 85:211–218

Yamaguchi T, Sato M, Hashihama F, Kato H and others (2021) Longitudinal and vertical variations of dissolved labile phosphoric monoesters and diesters in the subtropical North Pacific. Front Microbiol 11:570081

Zhou YP, Zhang YM, Li FF, Tan LJ, Wang JT (2017) Nutrients structure changes impact the competition and succession between diatom and dinoflagellate in the East China Sea. Sci Total Environ 574:499–508

Zhou ZX, Yu RC, Sun CJ, Feng M, Zhou MJ (2019) Impacts of Changjiang River discharge and Kuroshio intrusion on the diatom and dinoflagellate blooms in the East China Sea. J Geophys Res Oceans 124:5244–5257

*Editorial responsibility: Steven Lohrenz, New Bedford, Massachusetts, USA*
*Reviewed by: 3 anonymous referees*

*Submitted: May 21, 2022*
*Accepted: August 11, 2022*
*Proofs received from author(s): September 30, 2022*